

## Edge cracks in plastically deforming surface grains

Viggo Tvergaard<sup>a</sup>, Y. Wei<sup>b</sup>, J.W. Hutchinson<sup>b,\*</sup>

<sup>a</sup>*Department of Solid Mechanics, Technical University of Denmark, DK-2800 Lyngby, Denmark*

<sup>b</sup>*Division of Engineering and Applied Sciences, Harvard University, Cambridge, MA 02138, USA*

(Received 16 August 2000; revised and accepted 22 March 2001)

**Abstract** – A selection of surface crack problems is presented to provide insights into Stage I and early Stage II fatigue crack growth. Edge cracks at 45° and 90° to the surface are considered for cracks growing in single crystals. Both single crystal slip and conventional plasticity are employed as constitutive models. Edge cracks at 45° to the surface are considered that either (i) kink in the direction perpendicular to the surface, or (ii) approach a grain boundary across which only elastic deformations occur. © 2001 Éditions scientifiques et médicales Elsevier SAS

### 1. Introduction

For some rather pure metals, persistent slip bands (PSBs) develop in single crystals when they are subjected to cyclic loading (Ma and Laird, 1989; Pedersen, 1990). In such cases the development of small fatigue cracks is observed at the PSBs, usually along one of interfaces between the band and the surrounding crystal. Nucleation of these cracks is thought to be connected with the build-up of local stress concentrations, resulting from the development of extrusions and intrusions where the PSB intersects the surface of the crystal. The density of these small cracks is comparable to that of the PSBs, which may be as large as hundreds per centimeter (Ma and Laird, 1989). Most of the cracks appear to arrest and remain innocuous, while a few may grow large enough to become full fledged fatigue cracks. Structural polycrystalline metal alloys generally do not form PSBs, nevertheless, the early stage of fatigue crack initiation is thought to be qualitatively similar in that it is driven by highly localized irreversible plasticity. Thus, small cracks undergo Stage I growth along favorably oriented primary slip planes or microstructural features at approximately 45° to the surface. Most of these small cracks arrest, but a few continue into Stage II, change growth direction, and become small dominantly mode I cracks (Miller, 1993; McDowell, 1996).

In a recent paper Hutchinson and Tvergaard (1999) have investigated edge cracks in single crystals in order to study Stage I fatigue cracks, where the crack orientation is controlled by the slip direction. In that study slip was assumed to occur along planes inclined at 45° to the surface, and slip was modeled as elastic-perfectly plastic. In some cases slip was limited to a persistent slip band on one side of the crack, while in other cases slip was not confined. Studies were carried out for mixed mode conditions of small and large scale yielding. In small scale yielding, mixed mode elastic K-field displacements were prescribed as boundary conditions at an outer circular boundary of the region analyzed, while the full edge crack geometry was analyzed in large scale yielding. In these studies the focus was on crack tip opening and sliding displacements, as these measures are likely to be central in any extension of fatigue crack growth to small cracks and to formulations more

---

\* Correspondence and reprints.

E-mail address: hutchinson@husm.harvard.edu (J.W. Hutchinson).

fundamental than those based on elastic stress intensity factors. The analyses were used to obtain a parametric understanding of the effect of crack length relative to PSB width, as well as the effects of a barriers to slip. Both monotonic loading and cyclic loading were analyzed. For the case where the assumption of small scale yielding applies and where slip in the crystal is not confined, a very useful, simple conversion from monotonic to cyclic loading results was discussed.

The present paper continues the study initiated in the earlier paper. First, results are presented for edge cracks in single crystal grains oriented at both  $45^\circ$  and  $90^\circ$  to the surface using constitutive models based on slip in single crystals. The importance of crystal orientation is explored and so is the efficacy of modeling the crystal using isotropic plasticity. The transition from Stage I to Stage II is investigated by considering the kinking of the  $45^\circ$  crack in a direction perpendicular to the surface. The second part of the paper concerns a fatigue crack approaching a grain boundary which constrains the zone of plasticity at the tip. The focus is on structural alloys where PSBs are not observed, but where Stage I fatigue cracks tend to initiate in surface grains with favorably oriented slip planes. A specimen under cyclic loading is analyzed, with an edge crack penetrating into a surface grain. This surface grain is elastic–plastic, while the surrounding grains in the specimen are assumed to remain elastic. The constraint as the crack tip approaches the grain boundary is thus likely to overestimate the effect of misorientation, but it should nevertheless indicate the effect such a barrier has to small crack growth. The surface grain slip is represented by two sets of slip planes, each inclined at  $45^\circ$  to the surface. The grain contains a single surface crack parallel to one of the sets of slip planes. For sufficiently small cyclic stress levels with no interaction between the plastic zone and the grain boundary, this model problem reduces to conditions of small scale yielding analyzed earlier (Hutchinson and Tvergaard, 1999). The main interest here is in cases where the cyclic stress levels are sufficiently high, or the crack tip is sufficiently close to the grain boundary, so that the active cyclic plastic zone at the crack tip shows significant interaction with the elastic material surrounding the grain at the other side of the grain boundary.

## 2. Edge cracks: sensitivity to choice of plasticity model

In this section a selection of solutions for edge cracks envisioned to be in Stage I or early Stage II will be presented. The sensitivity of the crack tip displacements to slip orientation and other modeling options will be illustrated. The computations employ a two-dimensional finite element representation of the solid, which is assumed to be in a state of plane strain. The first of the edge crack geometries (see *figure 1*) consists of an edge crack of length  $a$  oriented at either  $45^\circ$  or  $90^\circ$  to the surface and stressed remotely by a tensile component  $\sigma$  acting parallel to the surface. The finite element model employs a square region with dimension which is many times the crack length and the normal traction is applied to the top and bottom faces of this region.

Two elastic–perfectly plastic constitutive laws are used to characterize the solid: single crystal slip and isotropic plasticity. Both versions assume isotropic elasticity with Young's modulus  $E$  and Poisson's ratio  $\nu$ . For single crystal slip, a slip system is assumed to be oriented at angle  $\beta$  to the free surface (see *figure 1*). In small strain plasticity, which is assumed in this study, slip on this one system is equivalent to the existence of two sets of slip planes, one with the orientation  $\beta$  and the other perpendicular to it. With  $\tau_Y$  as the critical shear stress required to cause yielding on the slip plane and with  $\tau$  as the resolved shear stress acting on the plane, the constitutive limitations on the slip increments  $\dot{\gamma}$  for a perfectly plastic crystal are:

$$\dot{\gamma} = 0 \quad \text{for } |\tau| < \tau_Y, \quad \dot{\gamma} \geq 0 \quad \text{for } \tau = \tau_Y, \quad \dot{\gamma} \leq 0 \quad \text{for } \tau = -\tau_Y. \quad (1)$$

Calculations will also be presented based on an isotropic plasticity model which uses the von Mises yield surface normalized such that under a pure shear stress  $\tau$  yield occurs when  $\tau = \tau_Y$  (i.e. the tensile yield stress is  $\sigma_Y = \sqrt{3}\tau_Y$ ).

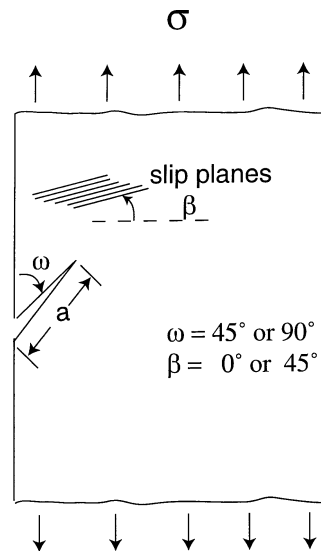


**Figure 1.** Edge cracks at  $\omega = 45^\circ$  and  $90^\circ$  under remote stressing. In the case of single crystal slip, the slip plane has orientation  $\beta = 0^\circ$  and  $45^\circ$ . Calculations for isotropic plasticity are also reported.



As in the earlier study, the emphasis will be on the opening and tangential displacements of the crack faces at the crack tip. These quantities seem to be the most obvious quantities to measure the intensity of deformation in the immediate vicinity of the crack tip and the most promising candidates for extending the current limitations of fatigue crack growth characterization. Let  $(\delta_n, \delta_t)$  denote the normal opening and tangential face displacements at the tip under monotonic loading and, similarly, let  $(\Delta\delta_n, \Delta\delta_t)$  denote the corresponding displacement changes under cyclic loading. The relative crack face displacements vary rather steeply as the crack tip is approached, and care must be taken to ensure the computed results are accurate. Here, the extrapolation scheme suggested by Hutchinson and Tvergaard (1999) has been used. With  $r$  as the distance to the tip at a point behind the tip, the equation for describing the variation of either of the relative face displacements is taken as:

$$\delta = Ar - B(r \ln r - r) + \delta(0), \quad (2)$$

where  $A$  and  $B$  are constants to be determined. The form (2) emerged from an analytic study of the near-tip behavior of cracks in single crystals by Saeedvafa and Rice (1992). It also pertains to the opening immediately behind the crack tip for the Dugdale model. While the general applicability of (2) has not been established, it does reflect the steep rate of change of the relative displacements found for the present models. To obtain the value at the tip,  $\delta(0)$ , three pairs of values of  $(r, \delta)$  from just behind the tip from the finite element calculation are used in (2) to evaluate  $A$ ,  $B$  and  $\delta(0)$ .

### 2.1. Cracks under monotonic and cyclic loads

Six cases are collected in *figure 2*, three for cracks at  $45^\circ$  to the surface and three for cracks perpendicular to the surface. For each crack orientation, three constitutive cases are considered: single crystal slip with systems oriented with  $\beta = 0^\circ$  and  $45^\circ$ , and isotropic plasticity. Moreover, results for both monotonic and cyclic loading have been presented. The emphasis in this section is not on large scale yielding effects (cf. Hutchinson and Tvergaard, 1999). The maximum stress applied under the monotonic history is  $\sigma_{\max}/(2\tau_Y) = 1/2$  such that the remote stress reaches exactly one half of the stress at yield and the crack remains just within the small scale

	$\beta=0^\circ$	$\beta=45^\circ$	Isotropic Plasticity
$\omega = 90^\circ$ 	$C_n = 1.30, C_t = 0$ $\Delta C_n = 0.63, \Delta C_t = 0$	$C_n = 0.60, C_t = 0$ $\Delta C_n = 0.32, \Delta C_t = 0$	$C_n = 1.31, C_t = 0$ $\Delta C_n = 0.66, \Delta C_t = 0$
$\omega = 45^\circ$ 	$C_n = 0.43, C_t = 0.27$ $\Delta C_n = 0.25, \Delta C_t = 0.13$	$C_n = 0.54, C_t = 0.24$ $\Delta C_n = 0.30, \Delta C_t = 0.13$	$C_n = 0.54, C_t = 0.29$ $\Delta C_n = 0.34, \Delta C_t = 0.15$

**Figure 2.** Numerical results for six cases – two crack orientations, each for three constitutive models.

yielding regime. The cyclic history applied to the specimen has the same maximum stress,  $\sigma_{\max}/(2\tau_Y) = 1/2$ , and zero minimum stress, such that  $\Delta\sigma/(2\tau_Y) = 1/2$ . It is important to mention that crack closure effects have not been emphasized in the present study. Under the cyclic history considered, the crack faces remain open over the entire cycle. Closure due to extrinsic effects such as crack face roughness, fatigue debris or plastic stretch left behind an advancing fatigue crack tip would affect the cyclic crack tip displacements.

For the monotonic cases, the crack tip displacements have been expressed as:

$$(\delta_n, \delta_t) = (C_n, C_t) \left( \frac{\sigma^2 a}{E \tau_Y} \right), \quad (3)$$

where the coefficients  $(C_n, C_t)$  calculated for the respective cases are included in *figure 2*. These are independent of the applied stress  $\sigma$  within the small scale yielding range. The corresponding expression for the changes in the crack tip displacements over a complete load cycle is:

$$(\Delta\delta_n, \Delta\delta_t) = (\Delta C_n, \Delta C_t) \left( \frac{\Delta\sigma^2 a}{E \tau_Y} \right), \quad (4)$$

where the  $(\Delta C_n, \Delta C_t)$  are also included in the figure. The behavior under the constant amplitude cyclic loading settles down to a “steady-state” after only several cycles in which the stress and crack face displacements no longer change from cycle to cycle at any given point in the cycle. Because the plastic zone size is much smaller under cyclic amplitude than that of the monotonic crack loaded to the same amplitude (by about a factor of four), the cyclic cases are well within the small scale yielding regime for the conditions under which the calculations have been carried out, i.e.  $\Delta\sigma/(2\tau_Y) = 1/2$ . It can be noted in *figure 2* that  $(\Delta C_n, \Delta C_t)$  are approximately 1/2 the respective values of  $(C_n, C_t)$ . This is a consequence of both the cyclic and the monotonic cases being within small scale yielding. In mode III, and also for the Dugdale model in mode I, the cyclic coefficients are exactly 1/2 their monotonic counterparts in small scale yielding (Rice, 1967). In these two problems the cyclic problem can be put into correspondence with the monotonic problem by doubling the yield stress,  $\tau_Y$ , reflecting that fact that the stress state traverses from one side of the yield surface to exactly the opposite side on a trajectory through the stress space wherever cyclic plastic deformation occurs. In plane strain, the trajectory is not expected to be as simple and ratio should not be precisely 1/2. Nevertheless, the present results indicate that this ratio is nearly 1/2, within the accuracy of the numerical evaluation of the coefficients.

Several observations can be made from the results collected in *figure 2*:

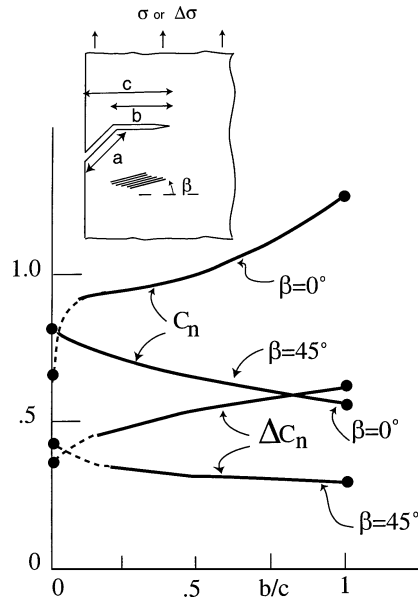


**Figure 3.** Coefficient specifying the opening crack tip displacements,  $\delta_n$  and  $\Delta\delta_n$ , for a kinked edge crack. The tangential components of the crack tip displacement are very small compared to the corresponding opening components and have not been presented.

(i) For cracks at  $90^\circ$  to the surface, the orientation of the slip system has a large effect on the crack tip opening. The system aligned at  $0^\circ$  (and therefore also at  $90^\circ$ ) is much more favorable to slip near the tip than that aligned at  $45^\circ$  (and also at  $-45^\circ$ ), and the coefficients  $C_n$  and  $\Delta C_n$  are correspondingly about twice as large. The coefficients from the isotropic plasticity model are very close to those for the slip system at  $0^\circ$ .

(ii) For cracks at  $45^\circ$  to the surface there are relatively small differences among the three constitutive models, although the normal opening component is about 20% smaller for the slip system oriented at  $0^\circ$  than as predicted for the other two models.

(iii) The behavior at the tip of the cracks at  $45^\circ$  is mixed mode with the opening component almost twice the tangential component. Moreover, the opening component is nearly as large as that for the mode I crack with the unfavorably oriented slip system (at  $45^\circ$ ), but it is less than one half the opening for the other two cases.

The results above are within the small scale yielding range. They may be re expressed in terms of stress intensity factors using:

$$K_I = 1.122\sigma\sqrt{\pi a}, \quad K_{II} = 0, \quad (5)$$

for the crack perpendicular to the edge, and by:

$$K_I = 0.705\sigma\sqrt{\pi a}, \quad K_{II} = 0.364\sigma\sqrt{\pi a}, \quad (6)$$

for the crack at  $45^\circ$  to the edge (Isida, 1979).

## 2.2. A $45^\circ$ edge crack transitioning to a $90^\circ$ mode I crack

Stage I cracks inclined to the surface transition to mode I, Stage II cracks as they grow longer. Here, an example will be presented which illustrates some features of this transition. The  $45^\circ$  edge-crack shown in the insert in *figure 3* has kinked with the segment at its end oriented at  $90^\circ$  to the applied stress. Now, the total

penetration of the crack perpendicular to the surface is denoted by  $c$ , the length of the kinked segment by  $b$ , and the length of the inclined segment by  $a$ . Two cases are shown in *figure 3*. One has the slip system oriented at  $45^\circ$  (and  $-45^\circ$ ) to the surface while the other has the system at  $0^\circ$  (and  $90^\circ$ ) to the surface. Plotted as a function of  $b/c$  in *figure 3* are the coefficients for the opening displacement,  $C_n$  and  $\Delta C_n$ , now defined as:

$$\delta_n = C_n \left( \frac{\sigma^2 c}{E \tau_Y} \right), \quad \Delta \delta_n = \Delta C_n \left( \frac{\Delta \sigma^2 c}{E \tau_Y} \right). \quad (7)$$

The coefficients for the tangential crack face displacements are not shown because they are extremely small over the entire range of  $b/c$  shown, except when  $b/c$  is very small. Thus, the transition to mode I following kinking takes place remarkably quickly. This suggests that microstructural features may readily overcome the small barrier to the transition to Stage I cracks. Included as solid end points for each of the curves in *figure 3* are the results for the appropriate limits from *figure 2*. The limit at  $b/c = 1$  pertains to the perpendicular edge-crack with the corresponding slip plane orientation. The limit when  $b/c = 0$  must coincide with results from *figure 2*, taking into account that  $c = a/\sqrt{2}$  when  $b = 0$ . The dashed segments of the curves in *figure 3* near  $b/c = 0$  indicate segments which are not resolved numerically.

### 3. An edge crack approaching a boundary surrounded by elastic grains

Grain boundaries can block incipient surface fatigue cracks such that their further growth is arrested, rendering them impotent. The misorientation of the slip systems across the boundary impedes plastic deformation ahead of the advancing crack. Here we model the limit where plasticity is confined to the grain containing a  $45^\circ$  edge crack. The slip system within the grain is also at  $45^\circ$ , with one slip plane parallel to the crack (and another perpendicular to the crack), providing the most favorable orientation for plasticity within the grain whether induced by the applied stress or by the crack. As sketched in *figure 4*, the surface grain is half-circular with radius  $R$ , and the crack emerges from the center point of the grain at the edge, and extends a distance  $a$  into the grain. The distance from the crack tip to the boundary is  $b = R - a$ . Elastic anisotropy mismatch may also impede the growth of a crack from one grain into another, but in this study elastic mismatch is not considered. A common Young's modulus  $E$  and Poisson's ratio  $\nu$  are assumed.

Cyclic stressing  $\sigma(t)$  is assumed to have minimum stress  $\sigma_{\min} = 0$  and maximum stress  $\sigma_{\max}$ . The emphasis here will be on small scale yielding conditions in the sense that the plastic zone is small compared to the crack length, but not necessarily small compared to the distance  $b$  separating the tip from the grain boundary. While there is general interest in small crack effects attributed to large scale yielding, small scale yielding covers a highly important range of cyclic loading. It applies, to a good approximation, to stress amplitudes satisfying  $\sigma_{\max} \leq 2\tau_Y$  corresponding to the onset of general yielding in the polycrystal (Hutchinson and Tvergaard, 1999). At any stage in the cycle, the mode I and II elastic stress intensity factors for the crack are given by (6).

By dimensional analysis, the two components of the crack tip displacement amplitudes can be written as:

$$\Delta \delta_n = \frac{\Delta K_I^2}{E \tau_Y} f_n \left( \frac{b}{R_p}, \frac{\tau_Y}{E} \right) \quad \text{and} \quad \Delta \delta_t = \frac{\Delta K_{II}^2}{E \tau_Y} f_t \left( \frac{b}{R_p}, \frac{\tau_Y}{E} \right). \quad (8)$$

Here,

$$R_p = \frac{1}{3\pi} \left( \frac{\Delta K_I}{4\tau_Y} \right)^2 \quad (9)$$

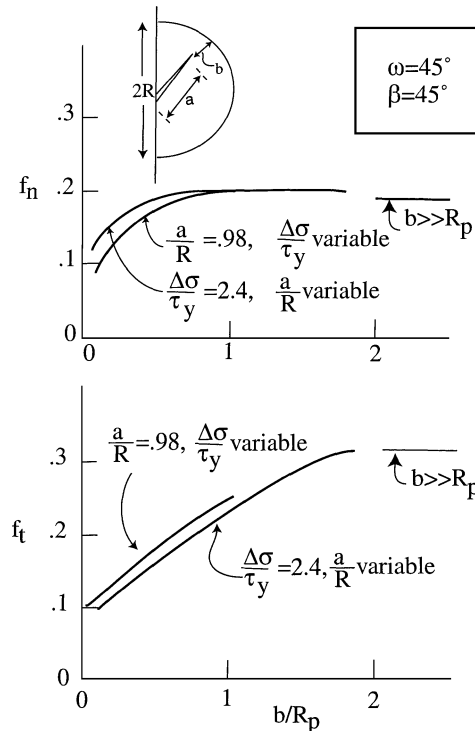


**Figure 4.** Edge crack at  $45^\circ$  contained within an elastic perfectly plastic grain surrounded by elastic grains. The slip system within the grain is oriented parallel to the crack (i.e. at  $45^\circ$  to the surface). Functions defining the crack tip displacements for the edge crack approaching the grain boundary.

is the reference length which scales with the active plastic zone size of the crack before it interacts with the boundary. The dependence on  $\tau_Y/E$  is weak, and  $\tau_Y/E = 0.002$  was used in all the calculations. Plots of  $f_n$  and  $f_t$  are given in *figure 4*. When the plastic zone does not reach the boundary (roughly  $b/R_p > 2$ ), the problem is the same as one addressed in Section 3.1. Then, by (7),  $f_n = 0.19$  and  $f_t = 0.31$ , strictly independent of  $b/R_p$  and  $\tau_Y/E$ . These limits are indicated in *figure 4*. The region outside the grain boundary constrains plastic deformation when  $b/R_p < 2$ , and the crack tip displacements are reduced relative to the unconstrained values. Two sets of calculations have been carried out producing the two sets of curves in *figure 4*. One was computed with  $a/R$  fixed at 0.98 by varying  $\Delta\sigma/\tau_Y$ , while the other set fixed  $\Delta\sigma/\tau_Y$  at 2.4 and varied  $a/R$ . The small differences between the two sets of curves, which should coincide, reflects inaccuracy in the numerical method. The drop off in the cyclic crack tip displacements becomes significant when  $b/R_p$  is reduced to 1/2. The limiting behavior of  $f_n$  and  $f_t$  as  $b/R_p$  approaches zero is not entirely clear. A finite opening displacement should be possible even with  $b = 0$ , since slip perpendicular to the tip is possible. However, the tangential component of opening at the tip is blocked by the grain boundary, and thus  $f_t$  is expected to approach zero as  $b/R_p$  approaches zero. The present numerical results are unable to resolve these two limits more accurately than displayed in *figure 4*.

#### 4. Concluding remarks

The results in the present paper provide trends in crack tip opening displacements for small Stage I and beginning Stage II cracks. Furthermore, they give some insight into the sensitivity of the predictions to the factors such as crystal orientation and constitutive modeling of the crystal. Characterization of growth under

cyclic loading for small cracks is likely to involve criteria making use of the cyclic crack tip displacements,  $\Delta\delta_n$  and  $\Delta\delta_t$ . Under mixed mode conditions both components will influence growth. For the 45° edge-crack the tangential component is approximately one half the amplitude of the opening component. Thus, while the mode I component is dominant, it seems likely that the superposition of the mode II component will be important in growth along a slip plane. In the case of the kinked 45° edge crack discussed in Section 3.2, it is remarkable that the crack tip is dominated by mode I behavior after only an exceptionally small kink (i.e.  $b/c \cong 0.1$ ). This suggests that it is microstructural features that probably determine the transition from Stage I to II. Finally, the 45° edge crack approaching a grain boundary across which no plasticity occurs provides an effective barrier for the termination of growth of a small Stage I crack. Crystal misorientation will have a similar, albeit a somewhat weaker, effect.

### Acknowledgments

The work of J.W.H. and Y.W. was supported in part by the AFSOR under Grant No. SA1542-22500 PG and in part by the Division of Engineering and Applied Sciences, Harvard University. In addition, Y.W. acknowledges support from the Chinese National Science Foundation.

### References

- Hutchinson, J.W., Tvergaard, V.T., 1999. Edge-cracks in single crystals under monotonic and cyclic loads. *Int. J. Fracture* 99, 81–95.
- Isida, M., 1979. Tension of a half space containing array cracks, branched cracks and cracks emanating from sharp notches. *T. Jpn. Soc. Mech. Eng.* 45, 306–317.
- Ma, B.T., Laird, C., 1989. Overview of fatigue behavior in copper single crystals: I, II and III. *Acta Metall.* 37, 325–336, 337–348, 349–355.
- McDowell, D.L., 1996. Basic issues in the mechanics of high cycle fatigue. *Int. J. Fracture* 80, 103–145.
- Miller, K.J., 1993. Materials science perspective of metal fatigue resistance. *Mater. Sci. Tech.* 9, 453–462.
- Pedersen, O.B., 1990. Mechanism maps for cyclic plasticity and fatigue of single phase materials. *Acta Metall. Mater.* 38, 1221–1239.
- Rice, J.R., 1967. Mechanics of crack tip deformation and extension by fatigue. *American Society of Testing Materials ASTM STP* 415, 247–309.
- Saeedvafa, M., Rice, J.R., 1992. Crack tip fields in a material with three independent slip systems: NiAl single crystal. *Modelling and Simulation in Materials Science and Engineering* 1, 53–71.